ACS APPLIED MATERIALS & INTERFACES

Research Article

www.acsami.org

Chirality-based Au@Ag Nanorod Dimers Sensor for Ultrasensitive PSA Detection

Lijuan Tang, Si Li, Liguang Xu,* Wei Ma, Hua Kuang, Libing Wang, and Chuanlai Xu

State Key Lab of Food Science and Technology, School of Food Science and Technology, Jiangnan University, Wuxi, Jiangsu 214122, People's Republic of China

Supporting Information

ABSTRACT: A novel biosensor for ultrasensitive detection of prostate-specific antigen (PSA) was established based on gold nanorod (Au NR) dimers assembly. The circular dichroism signal was significantly amplified by a silver shell depositing on the surface of the Au NR dimers. A low limit of detection of 0.076 aM and high specificity were observed within the range of 0.1 to 50 aM target PSA. The developed biosensor has the potential to serve as a general platform for the detection of cancer biomarkers.

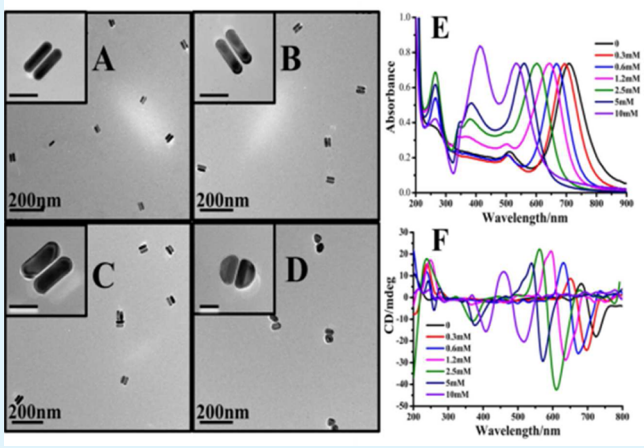

KEYWORDS: *Au@Ag nanorod dimers, chirality, PSA detection*

INTRODUCTION

Prostate-specific antigen (PSA), is a specific biomarker of prostate cancer, which has a high mortality rate.[1,2] PSA is found in both diseased and normal prostate cells.[3] In general, 4 ng/mL of PSA is the cutoff value in serum, and PSA levels above 4 ng/mL are generally thought to indicate a risk of prostate cancer.[4,5] Therefore, there is an urgent need to develop a method to monitor PSA levels to obtain an early and sensitive diagnosis of prostate cancer and to prevent cancer progression.

PSA detection is critical in the diagnosis of prostate cancer.[6] Enzyme-linked immunosorbent assay (ELISA) and radioimmunoassay are traditional methods for detecting PSA.[7,8] However, these approaches are based on antibodies, and are expensive, insensitive, time-consuming, laborious and difficult to use. To address these problems, novel detection strategies such as electrochemical methods, fluorescent assay and colorimetric assay have been developed.[9−11] However, electrochemical technology has limitations related to specificity and stability. The colorimetric method is fast and simple; however, sensitivity of this method is relatively low. Thus, it is very important to develop a simple, more sensitive and cost-effective assay for detecting PSA.

We have developed the sensors based on chiral nanomaterials for environmentally and biologically important targets detection.[12−16] In optical spectroscopy, molecular recognition-driven assembly of plasmonic nanoparticles into chiral structures can produce circular dichroism (CD) signals.[15] In general, the optical activity of the chiral assemblies with chiral cooperative interaction induced plasmonic CD greatly amplified.[17−20] Our research group has developed a number of chirality-based sensors used in trace detection. For example, chiral Au NP pyramids were used for endonuclease analysis[12] and a chiral pyramidal sensor was used to detect DNA.[21] Furthermore, the experimental chiroptical activity of side-by-side Au NR dimers has been reported by our group.[22] We previously found that coating the surface of Au NR dimers with a Ag shell can largely induce the E-fields enhancement. Inspired by these previous studies, we fabricated a chiral sensor consisting of side-by-side Au@Ag NR dimers to detect PSA.

In this study, a highly selective and sensitive chirality-based aptamer sensor for PSA detection was developed. As illustrated in Scheme 1, the PSA aptamer (DNA1) and its complementary fragment (DNA2) were coupled to the side of the Au NRs, respectively. Au NR-DNA1 was hybridized with Au NR-DNA2 to form the dimer probe following DNA hybridization in the absence of PSA. With the addition of PSA, the aptamer preferred to switch its configuration to combine with PSA, which caused the dimer to dehybridize to form single Au NRs. The higher the PSA concentration, the weaker the CD intensity. The CD intensity correlated well with the yield of

Received: February 8, 2015
Accepted: May 27, 2015
Published: May 27, 2015

DOI: 10.1021/acsami.5b01259
ACS Appl. Mater. Interfaces 2015, 7, 12708−12712

Scheme 1. Scheme of PSA Detection Based on Chirality Sensor of Au@Ag NR Dimers Building by Aptamer

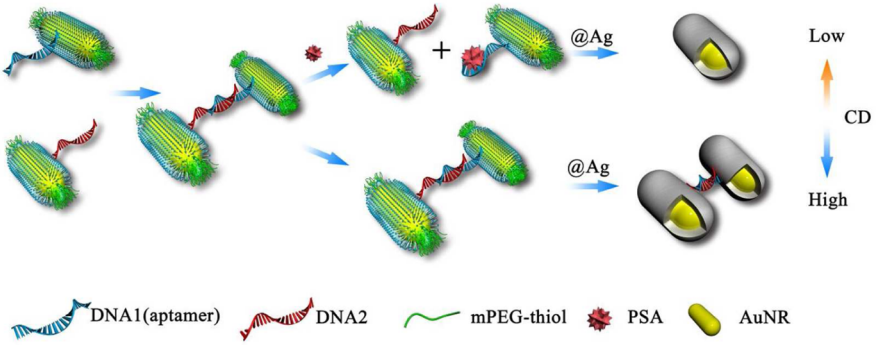

Au NR dimers in the sensing system, which allowed us to achieve ultrasensitive PSA detection.

MATERIALS AND METHODS

Materials and Reagents. The thiolated DNA aptamer was purchased from Shanghai Sangon Biological Engineering Technology & Services Co. Ltd. The aptamer was purified by high-performance liquid chromatography (HPLC) and suspended in deionized water obtained using a Milli-Q device (18.2 MΩ, Millipore, Molsheim, France). All other chemicals used in this work were obtained from Sigma-Aldrich.

The detailed sequences of the oligonucleotides are Aptamer (DNA1), 5′-SH-(T) 10-ATTAAAGCTCGCCATCAAATAGCTGC-3′;

Complementary (DNA2), 5′-SH-(T) 10-GCAGCTATTT-3′.

Au Nanorod (Au NR) Synthesis. *Synthesis of Au Seeds.*[23] Hydrogen tetrachloroaurate ($HAuCl_4$) (2.5 mL, 0.5 mM) and hexadecyltrimethylammonium bromide (CTAB) solution (2.5 mL, 0.2 M) were mixed together, then sodium borohydride ($NaBH_4$) (300 μL, 0.01 M) was added, and the solution was quickly mixed for 2 min and kept at 25 °C.

Growth of Au NR. $HAuCl_4$ (5 mL, 1 mM) was added to a CTAB (5 mL, 0.2 M) solution, $AgNO_3$ (0.12 mL, 4 mM) was then slowly added, and the solution was left to react for 5 min. Ascorbic acid (Vc) (70 μL, 0.079 M) was added into the above solution, and said solution was left to react for 2 min. Finally, the prepared Au seeds (12 μL) were added, vigorously stirred for 30 s and left at 25 °C for 2 h. The colloidal solution was centrifuged at 7000 rpm for 30 min. The precipitate was suspended in 5 mM CTAB solution, and the supernatants were removed. The Au NRs were characterized by transmission electron microscopy (TEM).

Au NRs Modification. To obtain side-by-side oriented Au NR dimers, the end facets of Au NRs were modified by thiolated PEG1000 (PEG) at a PEG/NR molar ratio of 20:1.[20] 50 μL Au NRs were mixed with Tris buffer (50 μL, 10 mM), and then 2 μL of PEG was added under vigorous stirring. After modification for 10 h, excess PEG was removed by centrifugation at 7000 rpm for 5 min, and the precipitate was dissolved in 100 μL of CTAB−Tris buffer. The PEG-modified Au NRs were then modified by 2 μL of DNA1 or DNA2. Following incubation for 12 h, excess DNA was removed by centrifugation (three times) at 7000 rpm for 5 min and suspended in 50 μL of CTAB−Tris buffer and characterized by dynamic light scattering (DLS). The CTAB coated on the surface of Au NRs formed a thin bilayer, which serves not only as the supporting electrolyte but also as the stabilizer for the nanoparticles, to prevent their further aggregation.

Fabrication of Side-by-Side Oriented Au NR Dimers and Synthesis of Au@Ag NR Dimers. Au NR-DNA1 (50 μL) and AuNR-DNA2 (50 μL) were mixed at a molar ratio of 1:1 and incubated for 8 h. The NR pairs were formed in CTAB−Tris buffer (10 mM Tris−HCl, 5 mM CTAB, 0.25 M NaCl).

Au NR dimers (100 μL) were centrifuged at 7000 rpm for 5 min and the precipitate was suspended in CTAB (200 μL, 20 mM) solution. Then, $AgNO_3$ (20 μL, 10−0.1 mM), Vc (10 μL, 0.1 M) and NaOH (20 μL, 10 mM) were sequently added. After reacting for 5 min, the mixtures were centrifuged at 6000 rpm for 5 min. The precipitate was then dissolved in deionized water (200 μL). The thickness of the Ag shell was adjusted by the addition of the concentrations of $AgNO_3$. TEM, ultraviolet−visible (UV−vis) and CD spectroscopy were used to analyze these products.

Measurement of the PSA-based Chiral Sensor. 50 μL of Au NR-DNA1 was mixed with 50 μL of Au NR-DNA2 in CTAB−Tris buffer (10 mM Tris−HCl, 5 mM CTAB, 0.25 M NaCl). After gentle shaking for 3 min, 1 μL of PSA at various concentrations was added to the above solutions, resulting in final concentrations of 0, 0.1, 0.5, 1, 5, 10 and 50 aM, respectively. The solutions were then incubated for 8 h at 37 °C. The reacted mixture was then coated with the Ag shell under optimized conditions. TEM, UV−vis and CD spectroscopy were used to monitor the disassembly.

Instrumentation. TEM images were obtained using a JEOL JEM-2100 operating at an acceleration voltage of 200 kV. All UV−vis spectra were acquired using a UNICO 2100 PC UV−vis spectrophotometer and processed with Origin Lab software. The DLS data were measured using a Zetasizer Nano ZS system (Malvern) with a 632.8 nm laser. The chirality of the nanostructures was characterized by MOS-450/AF circular dichroism.

RESULTS AND DISCUSSION

Characterization of Au NRs and the Conjugation of Au NR-DNA. The Au NRs with length/diameter of 43 nm/13 nm were synthesized by the seed growth method.[23] As shown in Figure S1A of the Supporting Information, the Au NRs had uniform morphology and good dispersity. To assemble side-by-side Au NR dimers, thiol-modified polyethylene glycol 1000 (PEG) was used to block the end facets of Au NRs at a PEG/NR molar ratio of 20:1. DNA1 and DNA2 were subsequently coupled with the side facets of NR at a DNA/NR molar ratio of 20:1. The hydrodynamic diameter (D_h) of Au NRs before and after DNA conjunction was measured by DLS. Figure S1B of the Supporting Information shows that the D_h of Au NR-DNA was longer than the naked Au NRs, which demonstrated that DNA was successfully modified onto the surface of the Au NRs. The number of DNA1 and DNA2 coupled on NRs was calculated to be 1.2 ± 0.3 and 1.1 ± 0.1, respectively. This indicated that approximately single-stranded DNA coupled to one NR could effectively guarantee the formation of NR dimers. The addition of thiol modified DNA leads to the side surface modification of NRs and therefore to form the side-by-side NR dimers, while thiolated PEG modified on the end sites of Au NRs to stabilize them in solutions.

Optimization of the Ag Shell Thickness of Au@Ag NR Dimers. After DNA1 and DNA2 were successfully modified onto the side surface of the Au NRs, the Au NR-DNA1 and Au NR-DNA2 were mixed at a molar ratio of 1:1 to assembly of Au

DOI: 10.1021/acsami.5b01259
ACS Appl. Mater. Interfaces 2015, 7, 12708−12712

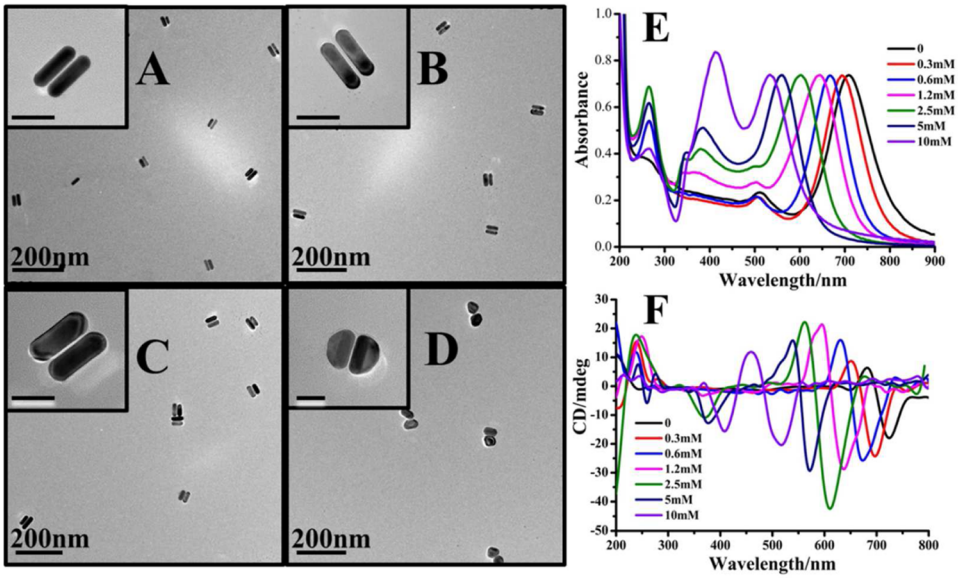

Figure 1. Au@Ag NR dimers with different Ag shell thickness by adding various concentrations of $AgNO_3$ in the range of 0 to 10 mM. (A,B,C,D) Representative TEM images of adding 0, 0.6, 2.5 and 10 mM $AgNO_3$, respectively. (E) Ultraviolet−visible (UV−vis) spectra. (F) CD spectra.

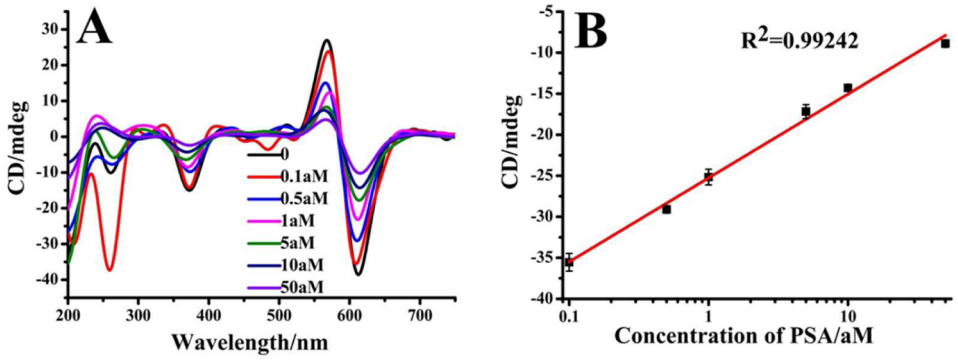

Figure 2. (A) CD spectral under different concentrations of PSA, and the concentrations of PSA were 0, 0.1, 0.5, 1, 5, 10 and 50 aM. (B) Standard curve of the determination of target PSA.

NR dimers. The NR pairs were then coated with additional Ag shell to yield Au@Ag NR dimers. To obtain the highest CD signal, the Ag shell thickness of Au@Ag NR dimers was optimized by adding different concentrations of $AgNO_3$. As shown in Figure 1A,B,C,D, the thickness of the Ag shell increased with increasing concentration of $AgNO_3$ from 0 to 10 mM. Moreover, Figure 1E shows the effect of the Ag shell on the surface plasmon resonance (SPR) of the Au NRs. The longitudinal LSPR gradually blue-shifted from 710 to 533 nm as the concentration of $AgNO_3$ increased from 0 to 10 mM. It should be noted that the LSPR of Ag gradually red-shifted and became stronger as the Ag shell became thicker. The CD signals of Au@Ag NR dimers with various Ag shell thicknesses were compared, in which the CD intensity increased initially, and then decreased with increasing Ag shell thickness (Figure 1F). The CD intensity was the maximum when the concentration of $AgNO_3$ was 2.5 mM. At this Ag shell thickness (6.89 nm), the signal was approximately 4 times higher than that for bare Au NR dimers. Therefore, 2.5 mM $AgNO_3$ was chosen as the optimum concentration to obtain the maximum CD signal. It should be noted that we choose to coat the Ag shell on the as-formed Au NRs dimer because the Ag shell can significantly reduce the gap between Au NRs. The gap has a large effect on the CD signal.

Construction of the Chiral Sensor for PSA Detection. A chiral sensor based on the high affinity of the PSA aptamer was used to detect PSA. The change of the ζ-potentials of gold nanorods suspensions before and after aptamer-modification is very small. And the ζ-potentials are +20.1 and +19.3 mV, respectively. The CD signals at various concentrations of PSA (0, 0.1, 0.5, 1, 5, 10 and 50 aM) are shown in Figure 2A. At low concentrations of protein,[24] the nonpsecific binding of PSA was eliminated by BSA blocking of low protein binding tubes and pipette tips with BSA (1.5 μM) blocking for 24 h in 10 mM CTAB−Tris buffer. With increased PSA concentration, the CD intensity at 610 nm decreased with a reduction in the number of dimers (Figure S2 of the Supporting Information). However, the UV−vis spectra at 610 nm were slightly changed (Figure S3 of the Supporting Information). A linear plot of the CD intensity at 610 nm versus the PSA concentration ranging from 0.1 to 50 aM was established with a correlation coefficient of 0.992 (Figure 2B). The limit of detection (LOD) was determined to be 0.076 aM. The LOD of PSA was determined based on a linear fit and the noise level of 3σ, where σ is the standard deviation of CD intensity at 610 nm measured at 0 aM

DOI: 10.1021/acsami.5b01259
ACS Appl. Mater. Interfaces 2015, 7, 12708−12712

PSA. The chiral signals originated from the chiral paired configurations, in which the overall geometry of NR dimers was determined by repulsive/attractive force. The fine balance of repulsive−attractive interaction coupled symmetrical breaking leads to thermodynamic preference of a specific enantiomer, which resulted in twisting of angled NR dimers toward either (−) or (+) enantiomer. The chiral oligonucleotide bridges provided the initial chiral preference force in the symmetrical breaking assemblies. The intrinsic chirality of organic coating of NR was also relevant in which Au NRs made by L-ascorbic acid reduction during their synthesis. When chiral PSA interacted with the chiral hybrid DNA−Au NRs dimers system, the interaction driven force can be multifold including PSA and aptamer recognition, chiral enantiomer coupled preference interactions related to the chiral spatial conformations. Additionally, the intense chiral signal in the Au NR dimer enantiomer excess gives rise to well and sensitive correlation with small amount of target PSA. It was also found that DNA2 is short, and we carried out the experiment very carefully (time and temperature control) and finally fabricated high yield Au NR dimers, during which the hybridization was done under relatively high salt concentration (0.25 M NaCl). A single DNA bridge formed in the Au NR dimer gap would help to achieve higher sensitivity.

The key factors attributed to the high sensitivity can be as follows. (1) Keep the most functional tail part of aptamer not to be hybridized to improve the recognition ability to the approaching PSA as competitive recognition mode; (2) the PSA could interact with only a small part of (−) enantiomers efficiently at low concentrations and induced the CD signal changes; (3) the highly intense chiral signal from the Au NR dimer with optimal silver shell coating further resulted in highly sensitive detection of PSA (0.076 aM).

The results demonstrated that the CD signal initially increased, and then decreased with increased Ag shell thickness. We infer that the spatial configuration of rod dimers could be changed to form the large dihedral angle to reduce the surface plasmonic resonance coupling effects and further decreased the intensity of CD signal as increasing the thickness of silver shells to reduce the electric repulsive of adjacent NRs. And the optimized Ag shell enhanced electrical field intensity to obtain the highest CD signal.

Specificity and Application of the Chiral Sensor. To confirm the specificity of this method, four chemicals (cysteine (Cys), glutamic acid (Glu), human serum albumin (HSA) and IgG), which are found in blood serum, were examined at a concentration of 1 mM. As shown in Figure 3, the CD signal at 610 nm for Cys, GLu, HSA and IgG was similar to that of the control without targets even at the high concentrations. However, the CD signal for PSA at the concentration of 1 aM was lower than the above control groups. Therefore, these results demonstrated that the designed biosensor was very specific and sensitive for PSA detection.

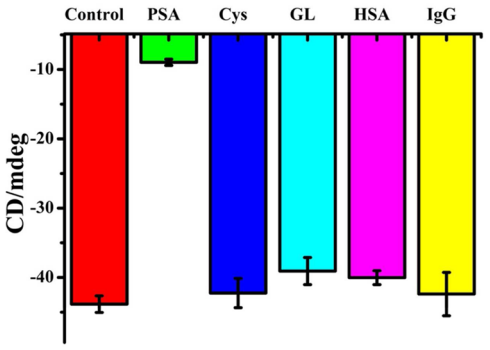

Figure 3. Evaluation of the selectivity of chirality sensor at different target analytes.

The applicability and reliability of this sensor were evaluated by testing three human blood samples, which were obtained from the Second Hospital in Wuxi, Provincial people's hospital. The concentrations of the three samples were 16.2, 46.7 and 5.88 pM, and were diluted to 16.2, 46.7 and 5.88 aM, respectively. As shown in Table 1, the detected concentration of PSA in solution was 15.8 ± 0.18, 47.2 ± 0.11 and 6.1 ± 0.14 aM, respectively. The experiment results of real samples indicate that the sensor has promising clinical applications.

Table 1. Practical Analysis of PSA in Serum Samples Based on Au@Ag NR Dimers

number of sample[a]	original concentration[b] (pM)	diluted concentration (aM)	detected concentration mean[c] ± SD[d]
1	16.2	16.2	15.8 ± 0.18
2	46.7	46.7	47.2 ± 0.11
3	5.88	5.88	6.1 ± 0.14

[a]Serum samples 1−3 are human sera, which are sampling from three healthy donors at the Second Hospital in Wuxi, China. [b]Original concentrations of PSA in the sera were determined by the standard clinical diagnostic assay (ADVIA Centaur, Siemens). [c]The mean of three experiments. [d]SD = standard deviation.

CONCLUSIONS

We demonstrated, for the first time, the highly selective and sensitive chirality sensor based on the aptamer-mediated Au NR dimer, in which an optimal Ag shell coating on the Au NR dimer was employed to enhance further the CD signal to enable ultrasensitive measuring PSA in patient sera. A LOD of 0.076 aM was obtained with the detection range of 0.1 to 50 aM target PSA based the CD spectra. Furthermore, excellent selectivity was confirmed by testing of other substances in the sera, and satisfactory detection in real blood samples was observed, which proved that this method has great potential for application in clinical diagnosis.

ASSOCIATED CONTENT

Supporting Information

Representative TEM image of dispersed Au NRs, and hydrodynamic size of Au NRs before and after DNA conjugation, representative TEM images of Au@Ag NR dimers with various PSA concentrations and UV−vis spectra of the sensing systems in the presence of various PSA concentrations. The Supporting Information is available free of charge on the ACS Publications website at DOI: 10.1021/acsami.5b01259.

AUTHOR INFORMATION

Corresponding Author

*L. Xu. E-mail: xuliguang2006@126.com.

Notes

The authors declare no competing financial interest.

DOI: 10.1021/acsami.5b01259
ACS Appl. Mater. Interfaces 2015, 7, 12708−12712

■ ACKNOWLEDGMENTS

This work is financially supported by the Key Programs from MOST (2012YQ09019410, 2012BAK17B10), and grants from Natural Science Foundation of Jiangsu Province, MOF and MOE (BE2013613, BE2013611).

■ REFERENCES

(1) Lilja, H.; Ulmert, D.; Vickers, A. J. Prostate-Specific Antigen and Prostate Cancer: Prediction, Detection and Monitoring. *Nat. Rev. Cancer* **2008**, *8* (4), 268−278.

(2) Wu, G.; Datar, R. H.; Hansen, K. M.; Thundat, T.; Cote, R. J.; Majumdar, A. Bioassay of Prostate-Specific antigen (PSA) Using Microcantilevers. *Nat. Biotechnol.* **2001**, *19* (9), 856−860.

(3) Chen, X.; Ba, Y.; Ma, L.; Cai, X.; Yin, Y.; Wang, K.; Guo, J.; Zhang, Y.; Chen, J.; Guo, X.; Li, Q.; Li, X.; Wang, W.; Wang, J.; Jiang, X.; Xiang, Y.; Xu, C.; Zheng, P.; Zhang, J.; Li, R.; Zhang, H.; Shang, X.; Gong, T.; Ning, G.; Zen, K.; Zhang, C. Y. Characterization of MicroRNAs in Serum: A Novel Class of Biomarkers for Diagnosis of Cancer and Other Diseases. *Cell Res.* **2008**, *18* (10), 997−1006.

(4) De la Rica, R.; Aili, D.; Stevens, M. M. Enzyme-Responsive Nanoparticles for Drug Release and Diagnostics. *Adv. Drug Delivery Rev.* **2012**, *64* (11), 967−978.

(5) Healy, D. A.; Hayes, C. J.; Leonard, P.; McKenna, L.; O'Kennedy, R. Biosensor Developments: Application to prostate-specific antigen detection. *Trends Biotechnol.* **2007**, *25* (3), 125−131.

(6) Wulfkuhle, J. D.; Liotta, L. A.; Petricoin, E. F. Proteomic Applications for the Early Detection of Cancer. *Nat. Rev. Cancer* **2003**, *3* (4), 267−275.

(7) Fenner, A. Prostate Cancer: Novel "Inverse Sensitivity" Enzyme-Linked Crystal-Growth Assay to Detect Ultralow PSA Levels. *Nat. Rev. Urol.* **2012**, *9* (7), 354.

(8) Graves, H. C.; Wehner, N.; Stamey, T. A. Ultrasensitive Radioimmunoassay of Prostate-Specific antigen. *Clin. Chem.* **1992**, *38* (5), 735−742.

(9) Kim, D. J.; Lee, N. E.; Park, J. S.; Park, I. J.; Kim, J. G.; Cho, H. J. Organic Electrochemical Transistor Based Immunosensor for Prostate Specific Antigen (PSA) Detection Using Gold Nanoparticles for Signal Amplification. *Biosens. Bioelectron.* **2010**, *25* (11), 2477−2482.

(10) Qu, F.; Li, T.; Yang, M. Colorimetric Platform for Visual Detection of Cancer Biomarker Based on Intrinsic Peroxidase Activity of Graphene Oxide. *Biosens. Bioelectron.* **2011**, *26* (9), 3927−3931.

(11) Wang, X.; Zhao, M.; Nolte, D. D.; Ratliff, T. L. Prostate Specific Antigen Detection in Patient Sera by Fluorescence-Free BioCD Protein Array. *Biosens. Bioelectron.* **2011**, *26* (5), 1871−1875.

(12) Hao, C. L.; Kuang, H.; Xu, L. G.; Liu, L. Q.; Ma, W.; Wang, L. B.; Xu, C. L. Chiral Supernanostructures for Ultrasensitive Endonuclease analysis. *J. Mater. Chem. B* **2013**, *1* (41), 5539−5542.

(13) Wang, L.; Zhu, Y.; Xu, L.; Chen, W.; Kuang, H.; Liu, L.; Agarwal, A.; Xu, C.; Kotov, N. A. Side-by-Side and End-to-End Gold Nanorod Assemblies for Environmental Toxin Sensing. *Angew. Chem., Int. Ed.* **2010**, *49* (32), 5472−5475.

(14) Wu, X.; Xu, L.; Liu, L.; Ma, W.; Yin, H.; Kuang, H.; Wang, L.; Xu, C.; Kotov, N. A. Unexpected Chirality of Nanoparticle Dimers and Ultrasensitive Chiroplasmonic Bioanalysis. *J. Am. Chem. Soc.* **2013**, *135* (49), 18629−18636.

(15) Xu, Z.; Xu, L.; Zhu, Y.; Ma, W.; Kuang, H.; Wang, L.; Xu, C. Chirality Based Sensor for Bisphenol A Detection. *Chem. Commun. (Cambridge, U. K.)* **2012**, *48* (46), 5760−5762.

(16) Yan, W.; Xu, L.; Xu, C.; Ma, W.; Kuang, H.; Wang, L.; Kotov, N. A. Self-Assembly of Chiral Nanoparticle Pyramids with Strong R/S Optical Activity. *J. Am. Chem. Soc.* **2012**, *134* (36), 15114−15121.

(17) Fan, Z. Y.; Govorov, A. O. Plasmonic Circular Dichroism of Chiral Metal Nanoparticle Assemblies. *Nano Lett.* **2010**, *10* (7), 2580−2587.

(18) Govorov, A. O. Plasmon-Induced Circular Dichroism of a Chiral Molecule in the Vicinity of Metal Nanocrystals. Application to Various Geometries. *J. Phys. Chem. C* **2011**, *115* (16), 7914−7923.

(19) Wen, T.; Hou, S.; Yan, J.; Zhang, H.; Liu, W.; Ji, Y.; Wu, X. L-Cysteine-Induced Chiroptical Activity in Assemblies of Gold Nanorods and Its Use in Ultrasensitive Detection of Copper Ions. *RSC Adv.* **2014**, *4*, 45159−45162.

(20) Hou, S.; Wen, T.; Zhang, H.; Liu, W.; Hu, X.; Wang, R.; Hu, Z.; Wu, X. Fabrication of Chiral Plasmonic Oligomers Using Cysteine-Modified Gold Nanorods as Monomers. *Nano Res.* **2014**, *11*, 1699−1705.

(21) Yan, W.; Xu, L.; Ma, W.; Liu, L.; Wang, L.; Kuang, H.; Xu, C. Pyramidal Sensor Platform with Reversible Chiroptical Signals for DNA Detection. *Small* **2014**, *10* (21), 4293−4297.

(22) Ma, W.; Kuang, H.; Xu, L.; Ding, L.; Xu, C.; Wang, L.; Kotov, N. A. Attomolar DNA Detection with Chiral Nanorod Assemblies. *Nat. Commun.* **2013**, *4*, 2689.

(23) Nikoobakht, B.; El-Sayed, M. A. Preparation and Growth Mechanism of Gold Nanorods (NRs) Using Seed-Mediated Growth Method. *Chem. Mater.* **2003**, *15* (10), 1957−1962.

(24) Koussa, M. A.; Halvorsen, K.; Ward, A.; Wong, W. P. DNA Nanoswitches: A Quantitative Platform for Gel-based Biomolecular Interaction Analysis. *Nat. Methods* **2015**, *12* (2), 123−6.

DOI: 10.1021/acsami.5b01259
ACS Appl. Mater. Interfaces 2015, 7, 12708−12712